

# Study of Microwave Performances of AlInN/GaN and AlGaN/GaN HEMT Devices up to 18GHz

G. Callet<sup>1,2</sup>, O. Jardel<sup>2</sup>, N. Sarazin<sup>2</sup>, E. Morvan<sup>2</sup>, M.A. DiForte-Poisson<sup>2</sup>, M. Oualli<sup>2</sup>, E. Chartier<sup>2</sup>, T. Reveyrand<sup>1</sup>,  
J-P. Teyssier<sup>1</sup>, S. Piotrowicz<sup>2</sup>, R. Quéré<sup>1</sup>, S.L. Delage<sup>2</sup>

<sup>1</sup>XLIM C2S2-UMR CNRS 6172, Université de Limoges, 7 rue Jules Vallès, 19100 Brive, France

<sup>2</sup>Alcatel-Thales 3-5 lab, 91460 Marcoussis, France

## Abstract

An intensive electrical characterization of AlInN/GaN HEMT devices is presented in this paper. The performances of these devices based on new material are compared with AlGaN/GaN HEMT devices, thanks to the measurement results and the extraction of small-signal models. Our study is based on 8x75μm devices processed by 3-5 Lab. Load-pull characterizations at 18 GHz will show the advantages of this technology at high frequencies.

## 1. Pulsed IV measurements

We present here the results of pulsed-IV measurements (pulse length 600ns, period 6μs) of the 8x75μm AlInN/GaN HEMT. These measurements avoid self-heating effects and highlight lag effects [1] when the quiescent bias points are changed. The comparison between  $V_{g\_bias}=0$  V and  $V_{g\_bias}=V_{pinch-off}$  shows the gate-lag (GL), and the comparison between  $V_{d\_bias}=0$  V and  $V_{d\_bias}>0$  V shows the drain-lag (DL). Thanks to this convention we can express gate-lag (1) and drain-lag (2) in percent using the following equations:

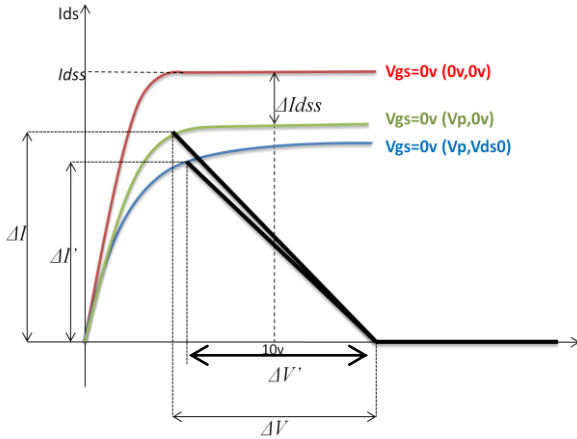


Fig. 1:  $V_{gs}=0V$  curves permitting to quantify lag at various quiescent bias: red  $V_{gs0}=0V$ ,  $V_{ds0}=0V$ ; green  $V_{gs0}=V_p$ ,  $V_{ds0}=0V$ ; blue  $V_{gs0}=V_p$ ,  $V_{ds0}=V_{bias}$

$$Gate\_lag(\%) = \frac{\Delta Id_{ss}}{Id_{ss0}} \Big|_{(V_{ds} > V_{knee})} \quad (1)$$

$$Drain\_lag(\%) = 1 - \frac{[\Delta V' \cdot \Delta I']_{(V_p, V_{ds0})}}{[\Delta V \cdot \Delta I]_{(V_p, 0)}} \quad (2)$$

One can notice that this figure of merit allow us to compare the lag of various devices but we observed differences of results from a bench to another, due to different pulse lengths for example. So in this paper we will only talk about devices measured in the same I(V) bench. Therefore we used this technique to measure the characteristics shown in figure 2.

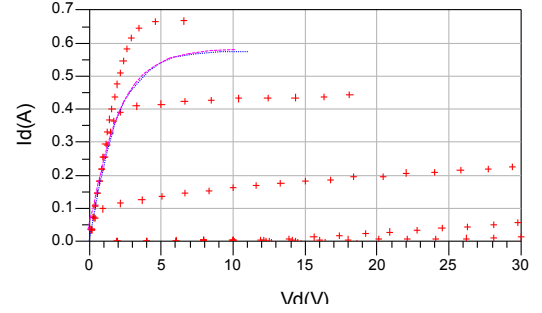


Fig 2. Pulsed I-V characteristics of AlInN based 8x75 device for different quiescent points: ( $v_{gs}=0v$ ,  $v_{ds}=0v$ ) red cross, curve at  $v_{g}=0v$  for ( $v_{gs}=-6v$ ,  $v_{ds}=0v$ ) blue dash, and curve at  $v_{g}=0v$  for ( $v_{gs}=-6v$ ,  $v_{ds}=20v$ ) solid line purple.

Table 1 summarizes the main I(V) characteristics of the AlInN/GaN device in comparison with a typical AlGaN/GaN one (same topology).

8x75μm	$I_{dss}$	DL	GL	$V_{pinchoff}$	$V_{knee}$	$V_{breakdown}$	$R_{on}(\Omega)$
AlInN	676 mA	≈0 %	14,5 %	-3,5V	3,5V	≈50V	4,1
AlGaN	730 mA	6 %	16,3 %	-6V	6V	≈90-105 V	6,4

Table 1. Comparison of IV characteristics, of AlGaN/GaN and AlInN/GaN devices

We can notice that the AlInN/GaN device has a lower  $I_{dss}$  than AlGaN/GaN counterpart, but presents a significant diminution of drain lag effects, which let us hope a good behavior for power applications. It is interesting to highlight too the low value of  $R_{on}$  (measured at  $V_{gs0}=0V$ ,  $V_{ds0}=0V$ ) for potentially switches applications.

The breakdown voltage (BVds) of AlInN devices is lower than the one of AlGaN devices. Then the  $V_{ds}$  biasing voltage commonly chosen for power applications with our AlGaN devices may be dangerous for AlInN ones as it reaches half of the BVds value. Hence, we choose a  $V_{ds}$  biasing voltage of 20V for AlInN devices instead of a typical voltage of 25V for AlGaN devices.

## 2. [S]-Parameters measurements

Fig 3 shows a comparison of the MSG/MAG gain of these two technologies at an AB-class bias point:  $V_{ds0}=20V$ ,  $I_{ds0}=150mA$ .



Fig 3. MSG/MAG gain of AlInN/GaN device (red) and, AlGaN/GaN device (blue).

We can see that the MSG/MAG transition (Rollet Factor=1) appears for a lower frequency in AlInN/GaN device (13GHz) instead of 26GHz for AlGaIn/GaN device. Nevertheless, the value of MSG gain is 2.5dB higher. In Table 2 we present a comparison of the intrinsic and extrinsic parameters of equivalent the small signal model. We remind the small signal model and the parameters we refer to in table 2 in figure 4.

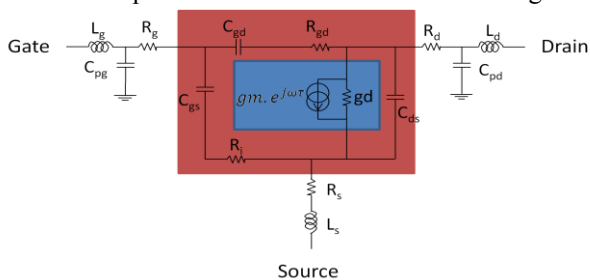


Fig 4. Small signal model of the devices, inside the red square the intrinsic parameters of the model and outside the extrinsic. The blue box represents the small signal current source.

8x75 $\mu$ m	Cgs	Cds	Cgd	Rgd	Ri	Gm	Gd	Tau
AlInN	1,35pF	180fF	85fF	38 $\Omega$	1,6 $\Omega$	240 mS	18 mS	1,73 ps
AlGaIn	619fF	160fF	70fF	17 $\Omega$	0,6 $\Omega$	109 mS	4,9 mS	1,88 ps
8x75 $\mu$ m	Rg	Lg	Cpg	Rd	Ld	Cpd	Rs	Ls
AlInN	0,85 $\Omega$	19pH	47fF	0,8 $\Omega$	42pH	92fF	0,85 $\Omega$	8,8pH
AlGaIn	0,75 $\Omega$	45pH	22fF	0,8 $\Omega$	89pH	83fF	0,65 $\Omega$	2,1pH

Table 2. Comparison of the intrinsic and extrinsic parameters of the small signal model of AlGaIn/GaN ( $v_{ds}=20V$ ,  $I_{ds}=150mA$ ) and AlInN/GaN devices ( $v_{ds}=20V$ ,  $I_{ds}=150mA$ )

The most important differences between the parameters of the small signal equivalent model of these devices are the Cgs capacitances and the transconductance Gm, which are nearly twice higher for AlInN/GaN.

We can explain it by reminding that the Cgs capacitance is directly proportional to transconductance Gm. The latter is by definition the slope of the drain current versus the gate pinch off voltage, and we can verify, in table 1, that the pinch off voltage of the AlInN/GaN device is actually twice lower than in the AlGaIn/GaN one.

### 3. Load-Pull measurements

In order to evaluate the power performances of AlInN/GaN components up to 18 GHz, we performed load-pull measurements in CW mode. The performances obtained for the optimal load impedance for power added efficiency (PAE) are presented in Fig. 4.

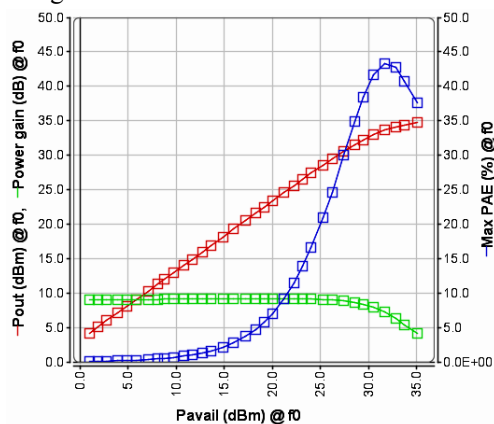


Fig 4. Power performances of AlInN/GaN at 18GHz, in red Pout (dBm), in green Power Gain (dB), in blue PAE (%).

These results are also compared to 8x75 $\mu$ m AlGaIn/GaN device. The power performances, of the two devices, are compared in table 3. The quiescent bias point is still  $V_{ds0}=20V$ ,  $I_{ds0}=150mA$  for AlInN/GaN and  $V_{ds0}=25V$ ,  $I_{ds0}=120mA$  for AlGaIn/GaN one. Performances are compared for both devices at the optimal impedance of maximum PAE.

8x75 $\mu$ m	PAE	Pout	Compression Gain	Zload	Fload
AlGaIn/GaN	33,7%	32,7dBm	3dB	9,5+15,8j	0,7/143 $^\circ$
AlInN/GaN	42,7%	34,1dBm	3dB	12,3+14j	0,6/148 $^\circ$

Table 3. Power performances at 18GHz at optimal impedances of maximum PAE.

We obtained an output power of 34.1 dBm (2.5W) which correspond to 4.3 W/mm with a PAE of 42.7 %. This relatively high value of PAE shows tacitly the low level of drain lag of these devices.

In the first paragraph, we explained a reliable way to quantify the lag effects of devices. In high power measurements we can also notice these effects. In the figure 6, we show a comparison of the average drain current versus the input power for the two technologies. Even if the quiescent bias currents are slightly different, we focus on the behavior of the drain current [3]. The main impact of the drain-lag effects is the slight current collapse observed for the AlGaIn based device, which is almost nonexistent for AlInN based one. The gate-lag effect is more reflected by the slope of this drain current curve in nonlinear functioning.

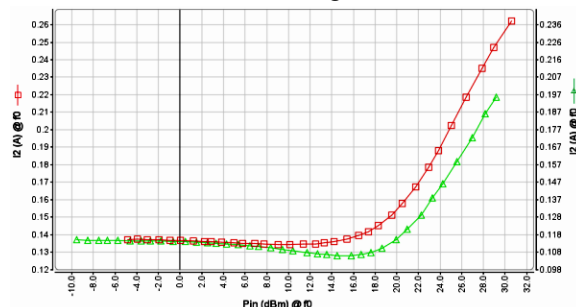


Fig 5. Average drain current versus input power, in red AlInN/GaN ( $V_{ds0}=20V$ ,  $I_{ds0}=150mA$ ), in green AlGaIn/GaN ( $V_{ds0}=25V$ ,  $I_{ds0}=120mA$ ).

We notice that measurements obtained in load-pull corroborate the results highlighted with the I(V) curves at  $V_{gs}=0V$ .

### 4. Conclusion

AlInN/GaN HEMT devices demonstrate interesting performances thanks to its free drain trapping effect. Very encouraging power performances were obtained at 18 GHz in CW mode with an output power of 34.1 dBm (4.3W/mm) and a PAE of 42.7%.

Actually we need complementary measurements at lower frequencies in order to validate the component for power wide-band applications.

The research leading to these results has received funding from Seventh Framework Programme FP7/2007-2011 under grant agreement n $^\circ$ 214610, project MORGaN.

[1] J.P. Teyssier, et al « 40GHz/150ns Versatile Pulsed Measurement System for microwave Transistor Isothermal Characterisation », IEEE MTT, December 1998.

[2] C. Charbonniaud, et al « Electrothermal and trapping effects characterisations », GAAS 2003, 6-7 oct, Munich 2003.

[3] O. Jardel, et al « An Electrothermal Model for ALGaIn/GaN Power HEMTs Including Trapping Effects to Improve Large-Signal Simulation Results on High VSWR », Microwave Theory and Techniques, IEEE Transactions on, December 2007.